Supplemental Material

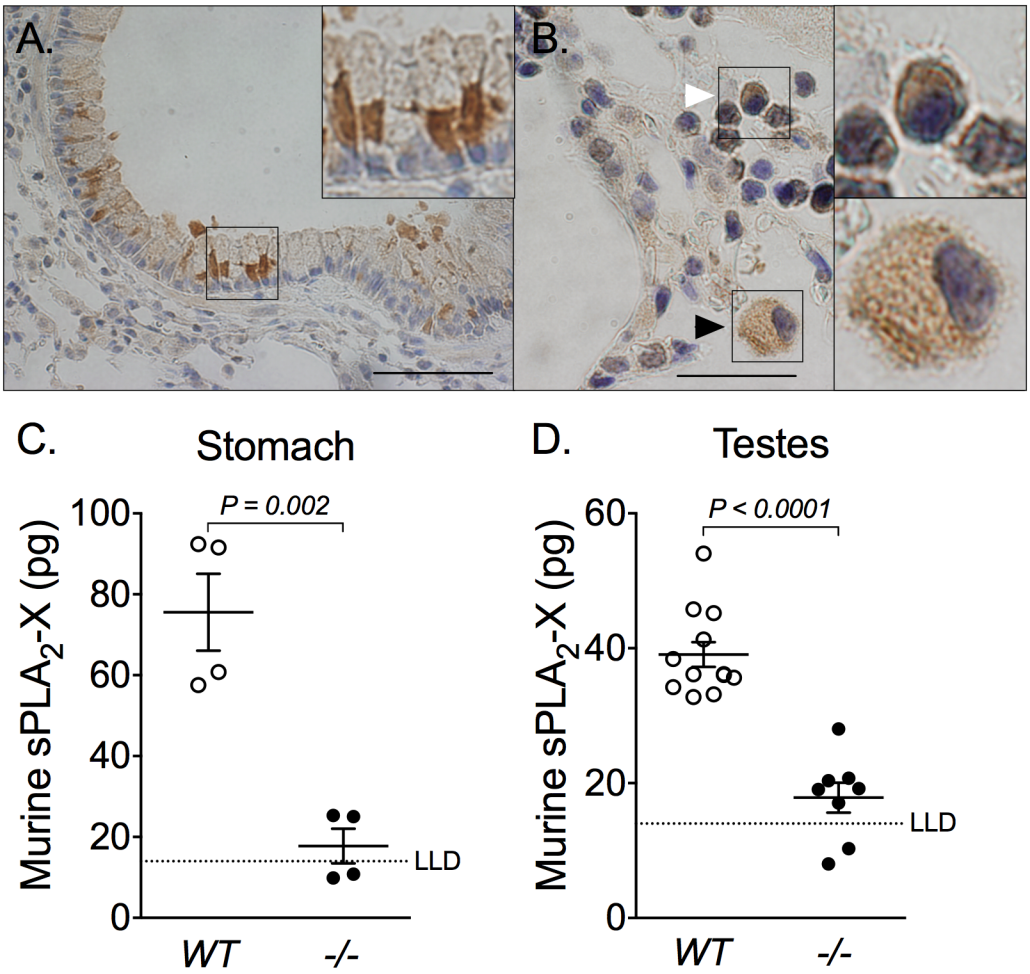

Supplemental Figure 1: Cellular localization of $sPLA_2$-X staining in the lung and confirmation of *Pla2g10* genetic ablation. Staining of *WT* lung tissue with an anti-$sPLA_2$-X antibody showing positive staining in (**A**) the airway epithelium (scale bar, 50 µm) and (**B**) alveolar macrophages (black arrowhead) and monocyte derived (recruited) macrophages (white arrowhead; scale bar, 20 µm). Insets show detailed staining of epithelium and macrophages. Quantitative assay of $sPLA_2$-X protein in (**C**) stomach (n = 4 mice/group) and (**D**) testes (n = 8 for *Pla2g10*$^{-/-}$ and 12 for *WT*) from *WT* and *Pla2g10*$^{-/-}$ mice confirming that global genetic ablation results in the lack of $sPLA_2$-X protein. Mean ± SEM, unpaired *t-test*.

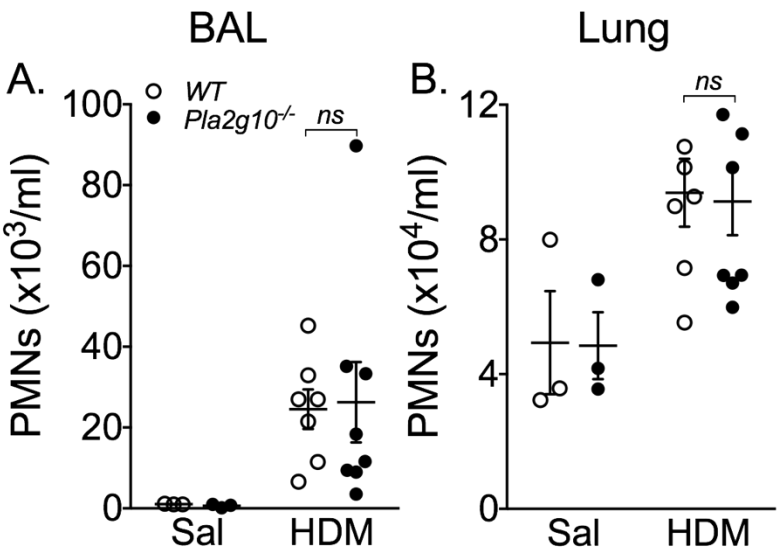

Supplemental Figure 2: Neutrophil concentrations in the BAL and lung. No differences in neutrophil influx were observed between *WT* and *Pla2g10*$^{-/-}$ mice in (**A**) BAL fluid or (**B**) lung tissue following sensitization and challenge with HDM (*n* = 3 mice/group for Sal, 7 mice for *WT* HDM and 8 mice for *Pla2g10*$^{-/-}$ HDM).

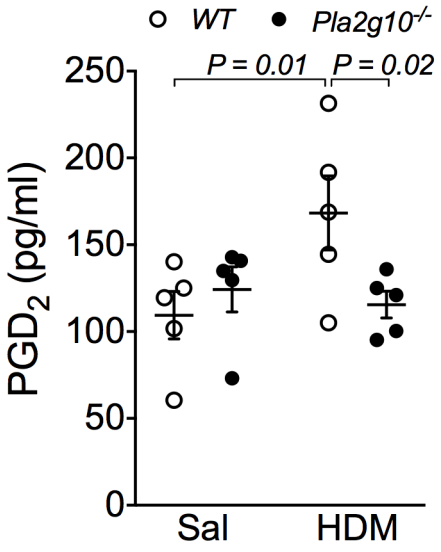

Supplemental Figure 3: Lack of *Pla2g10* alters PGD_2 production. Concentration of PGD_2 in BAL fluid from HDM-sensitized and challenged *WT* and *Pla2g10*$^{-/-}$ mice (*n* = 5 mice/group). Mean ± SEM, 2-way ANOVA with uncorrected Fisher's LSD.

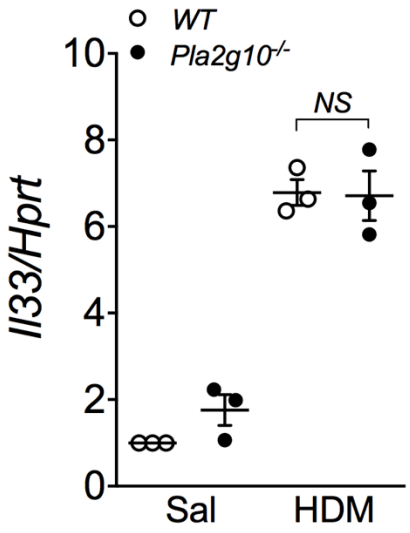

Supplemental Figure 4: Lack of *Pla2g10* does not affect IL-33 gene expression. Expression of *Il33* in lung tissue from HDM-sensitized and challenged *WT* and *Pla2g10*$^{-/-}$ mice (*n* = 3 mice/group). Mean ± SEM, 2-way ANOVA with uncorrected Fisher's LSD.

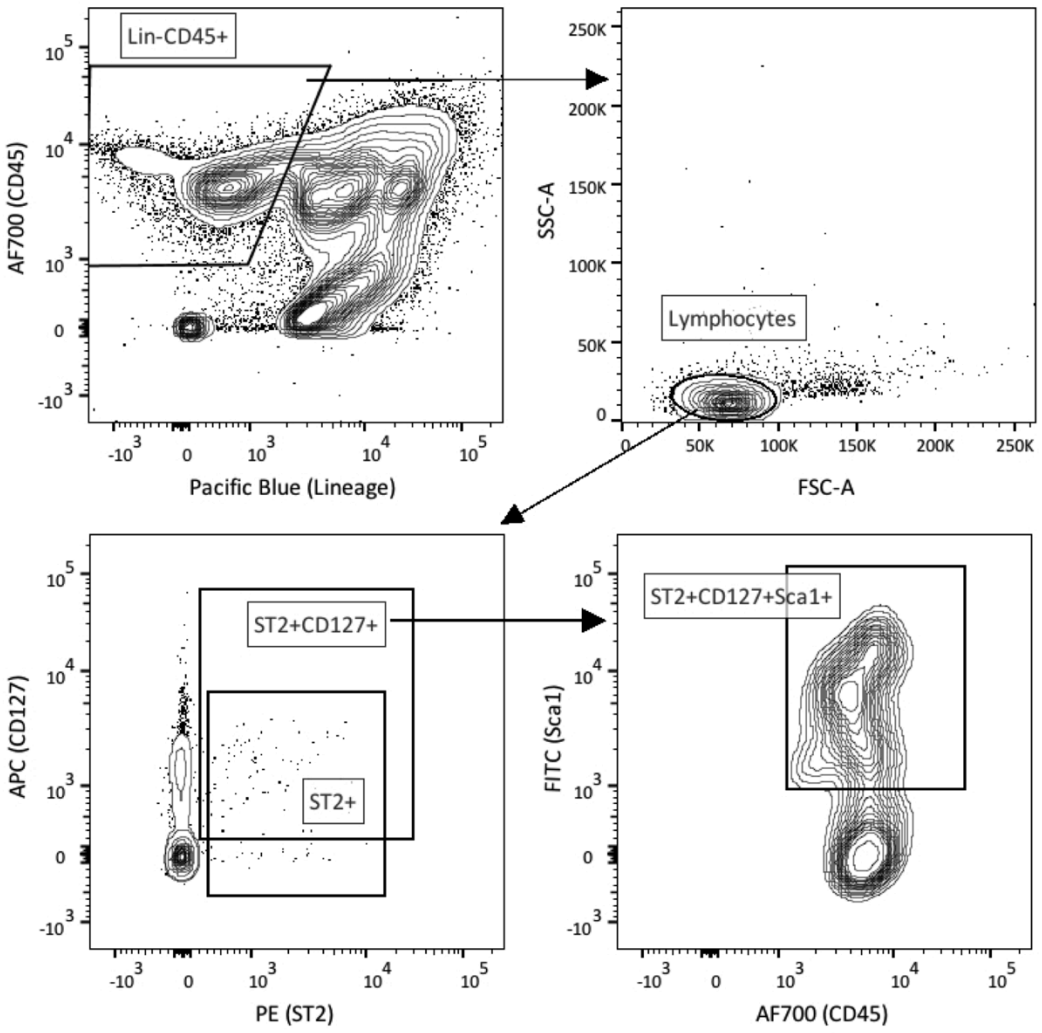

Supplemental Figure 5: Gating strategy for characterization of lung ILC2s. Lineage negative CD45 expressing (Lin^-CD45^+) cells were isolated and further gated by side and forward scatter area for lymphocytes. From the lymphocyte gate, Lin^- cells were further characterized as $ST2^+$, $ST2^+CD127^+$, or $ST2^+CD127^+Sca1^+$.

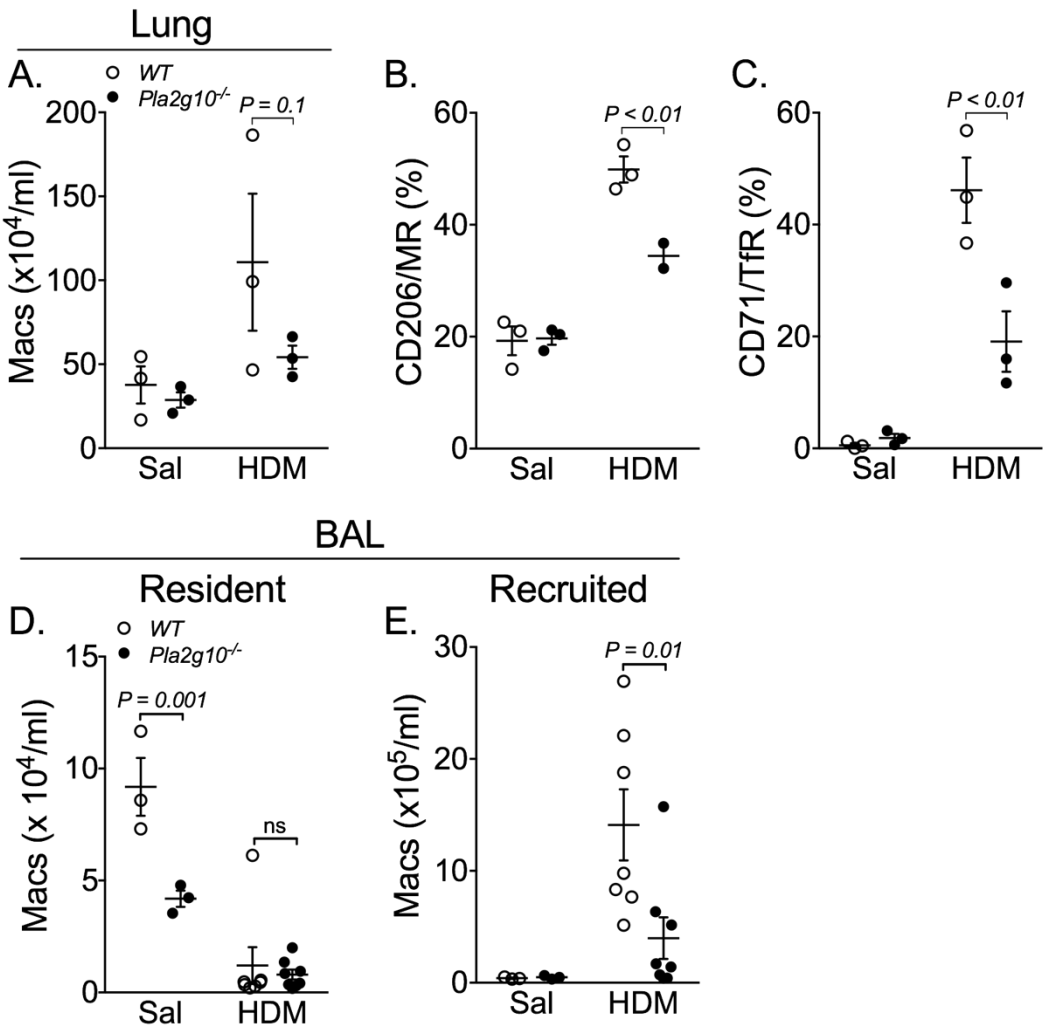

Supplemental Figure 6: Resident and recruited macrophage populations in lung tissue and BAL fluid following HDM exposure. (**A**) Concentration of macrophages in the lungs of *WT* and *Pla2g10*$^{-/-}$ mice (*n* = 3 mice/group). Mean ± SEM. (**B**) Percentages of CD206/MR^{+} macrophages and (**C**) CD71/TfR^{+} macrophages in the lungs of *WT* and *Pla2g10*$^{-/-}$ mice (*n* = 3 mice/group). Mean ± SEM. (**D**) Assessment of resident macrophages in the BAL fluid of *WT* and *Pla2g10*$^{-/-}$ mice (*n* = 3 mice/group for Sal, 7 mice for WT HDM and 8 mice for *Pla2g10*$^{-/-}$ HDM). Mean ± SEM. (**E**) Assessment of recruited macrophages in the BAL fluid of *WT* and *Pla2g10*$^{-/-}$ mice (*n* = 3 mice/group for Sal, 7 mice for WT HDM and 8 mice for *Pla2g10*$^{-/-}$ HDM). Mean ± SEM. Statistical significance was determined using 2-way ANOVA with uncorrected Fisher's LSD.

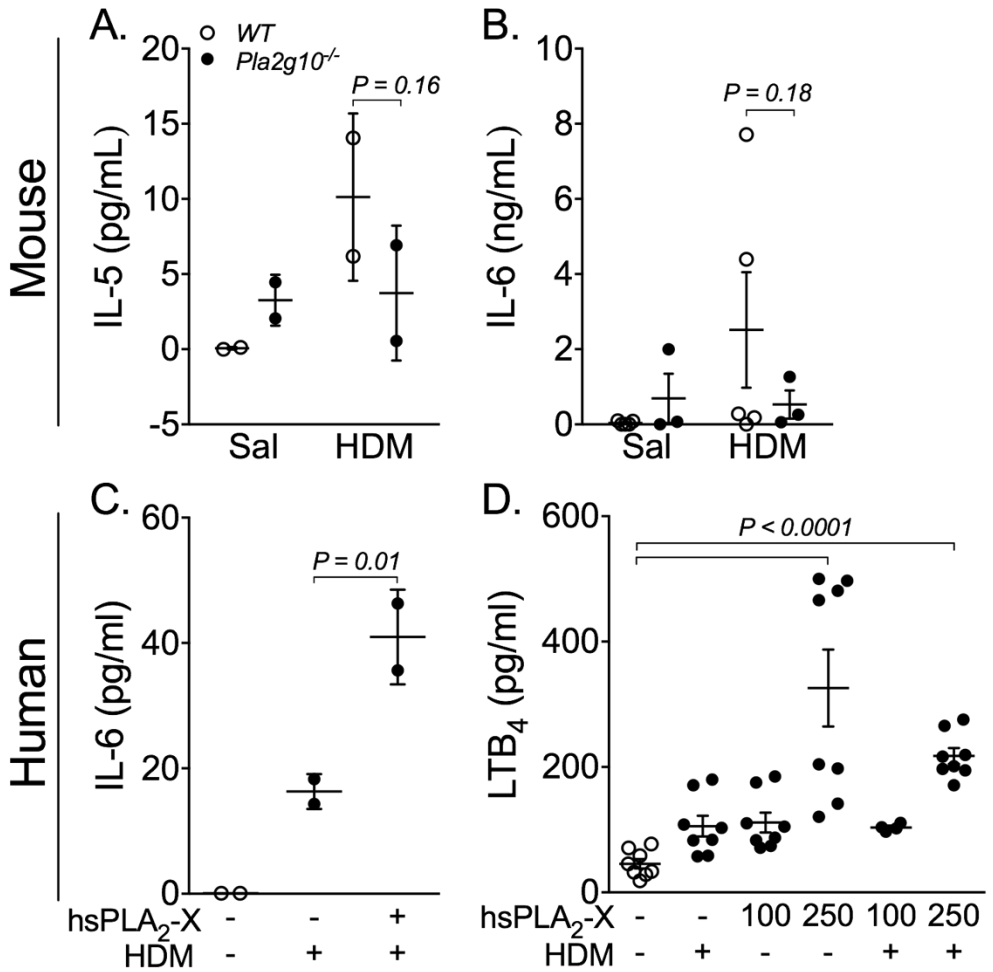

Supplemental Figure 7: Effects of $sPLA_2$-X on the activation of murine and human macrophages. (**A**) IL-5 and (**B**) IL-6 cytokine concentrations isolated from the lungs of *WT* and *Pla2g10*$^{-/-}$ murine macrophages following treatment with either saline or HDM (For IL-5: *n* = 2/group, mean ± SD; for IL-6: *n* = 5/group for *WT* and 3/group for *Pla2g10*$^{-/-}$, mean ± SEM). Human peripheral blood macrophages release (**C**) IL-6 and (**D**) LTB_4 in response to stimulation with HDM or recombinant human $sPLA_2$-X ($hsPLA_2$-X), though the effects on LTB_4 are not additive (For IL-6: *n* = 2/group, mean ± SD; for LTB_4, *n* = 4-8/group, mean ± SEM). Statistical analyses for panels **A** and **B**, 2-way ANOVA with uncorrected Fisher's LSD; for panel **C**, one-way ANOVA; for panel **D**, Kruskal-Wallis test.

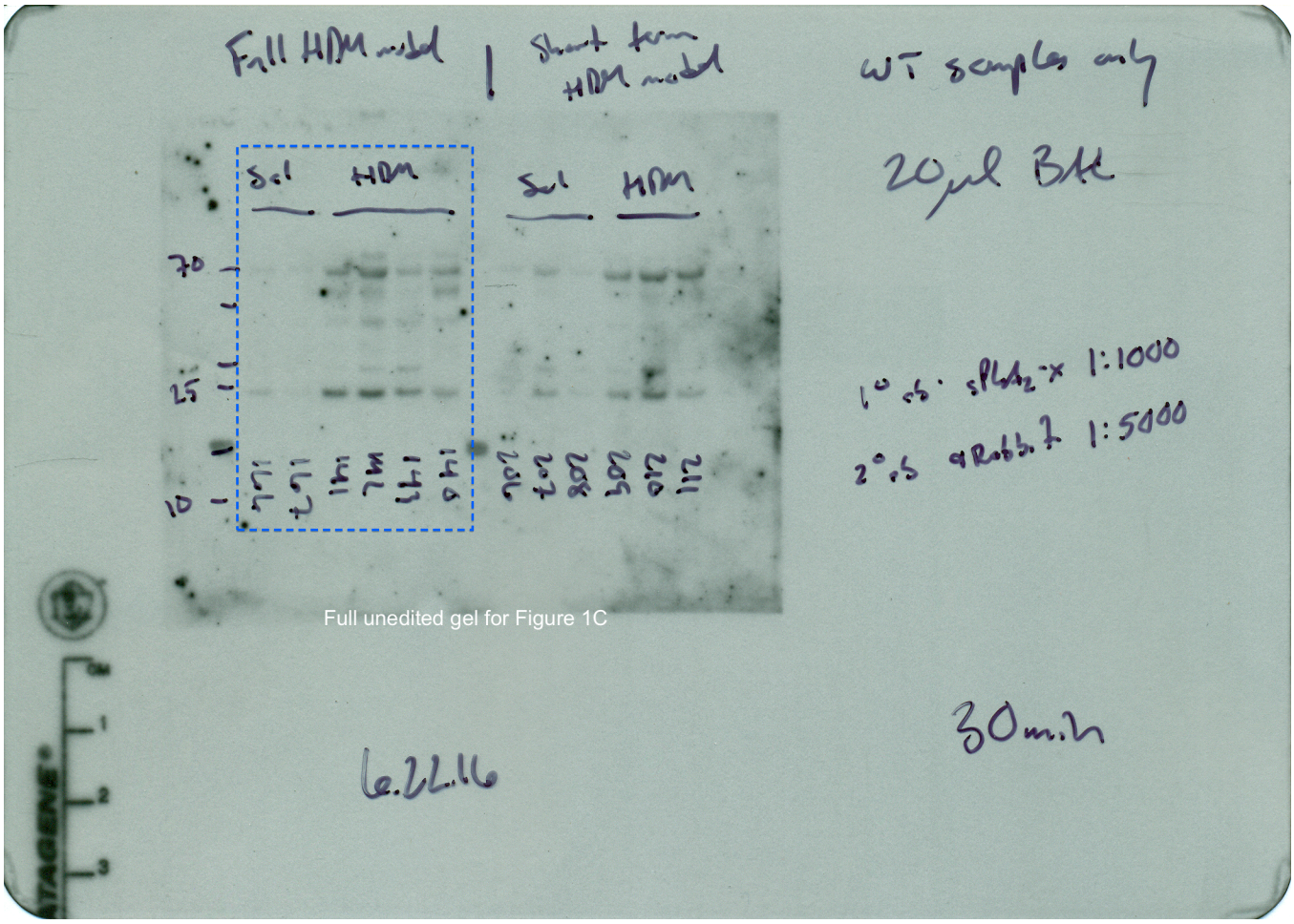

Full unedited gel for Figure 1C

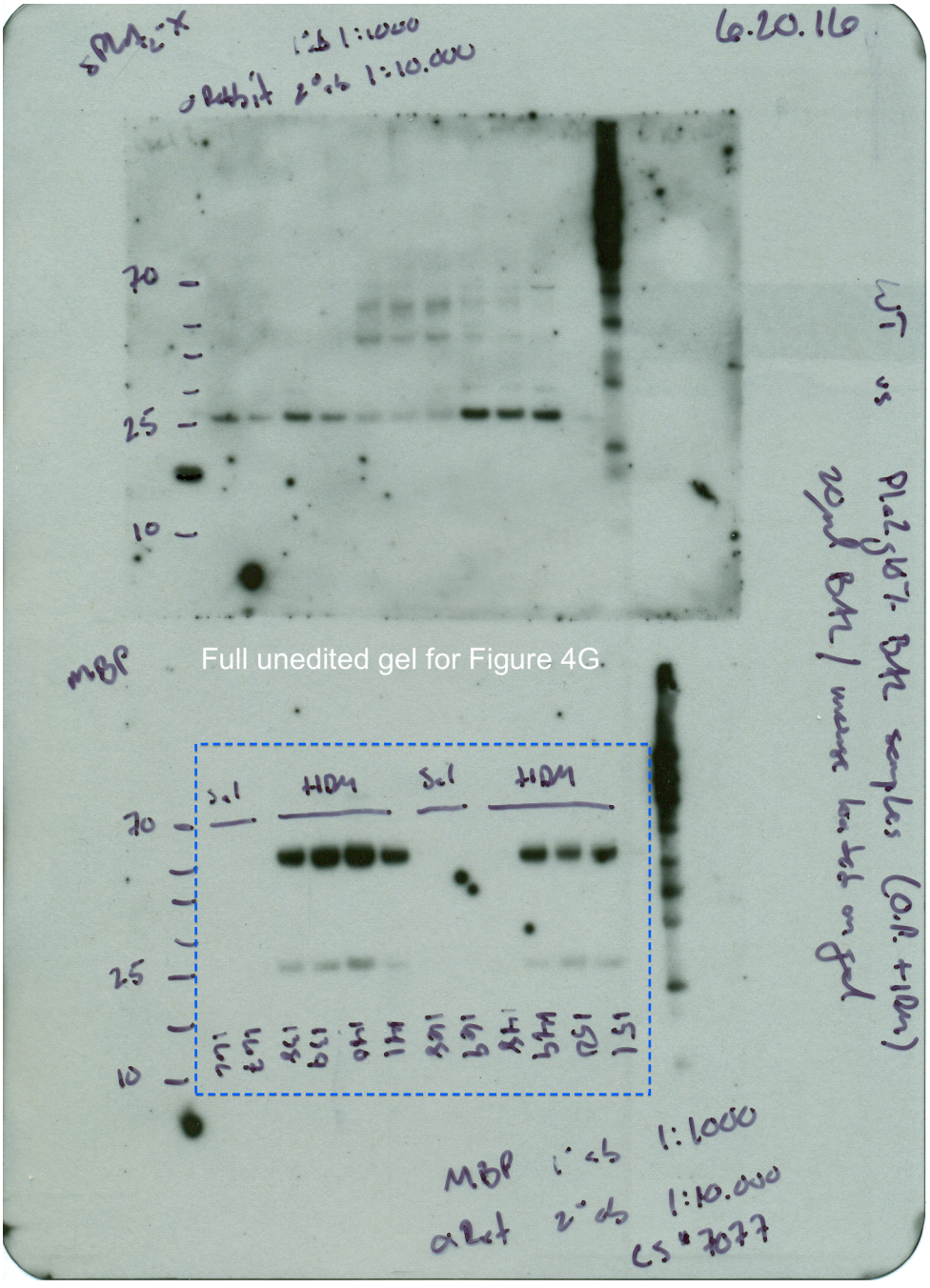

Full unedited gel for Figure 4G

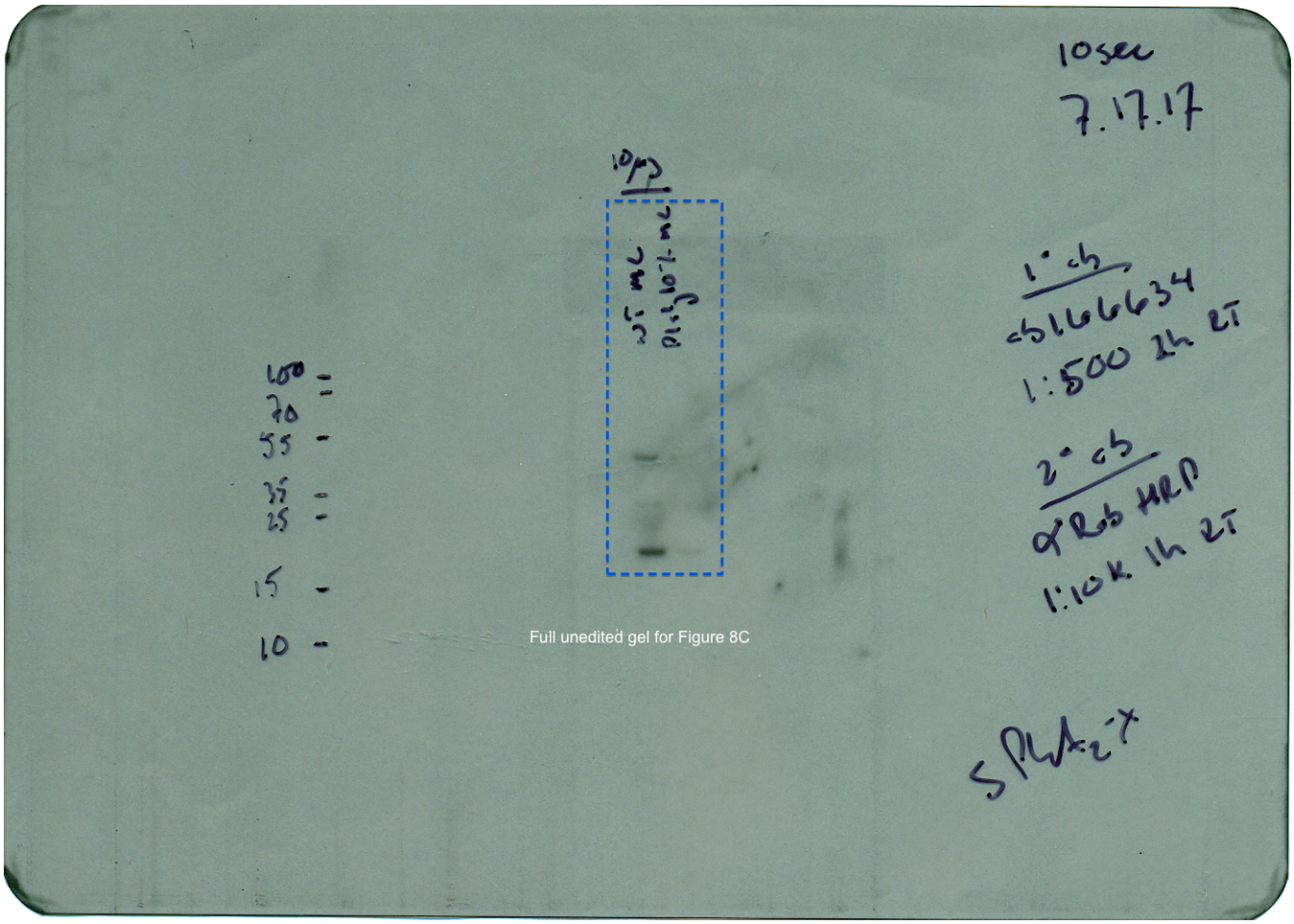

Full unedited gel for Figure 8C